Exposure of Portland-Limestone Cement – Metakaolin Paste to Cold Chloride-Sulfate Environment: NMR Spectroscopy Assessment of Structural Changes in Hydrated Phases and Relation to Chloride Ingress

Konstantinos Sotiriadis[1](✉), Anton Mazur[2], Peter Tolstoy[2], and Radek Ševčík[1]

[1] Institute of Theoretical and Applied Mechanics of the Czech Academy of Sciences, Prosecká 809/76, Prague 19000, Czechia
sotiriadis@itam.cas.cz

[2] Center for Magnetic Resonance, St. Petersburg State University, Universitetsky Pr. 26, St. Petersburg, Petergof 198504, Russia

Abstract. The effect of sulfates on chloride ingress and microstructure in Portland-limestone cement – metakaolin paste was studied. Crystalline and amorphous phases were investigated with X-ray powder diffraction and solid-state nuclear magnetic resonance spectroscopy. Free chlorides were determined with ion chromatography. The influence of metakaolin on the microstructure and chloride binding was highlighted by comparing the material with pure Portland-limestone cement paste. The results showed that the high Al content in metakaolin increased the chloride binding ability of the binder and Al incorporation in the C–S–H phase. Close to the surface, metakaolin admixture contributed in greater polymerization of the silicate chains of C–S–H, while larger amounts of unreacted clinker were observed, compared to deeper parts. At higher depths, chlorides bound in the form of Friedel's salt and free chlorides, were considerably reduced, attributed to refinement of the matrix. The presence of sulfates in the exposure solution affected chloride binding by inhibiting the formation of Friedel's salt and increasing free chlorides in the pore solution. Moreover, sulfates decreased the polymerization of the silicate chains in the C–S–H of the Portland-limestone cement – metakaolin paste and reduced the hydration of clinker in pure Portland-limestone cement paste.

Keywords: Portland-limestone Cement · Metakaolin · Chloride Ingress · Sulfate Attack · NMR Spectroscopy

A. Jędrzejewska et al. (Eds.): SynerCrete 2023, RILEM Bookseries 44, pp. 966–973, 2023.
https://doi.org/10.1007/978-3-031-33187-9_88

1 Introduction

Current trends in cement and concrete industry are directed towards the reduction of the overall environmental impact of cement production process, while maintaining proper performance characteristics of concrete. Portland-limestone cements with limestone content up to 15% by weight of cement, specified in the relevant European and American standards [1, 2], serve these goals as they significantly reduce clinker requirements. However, sulfate corrosion is of concern, because at cold and humid conditions they are vulnerable to the so-called thaumasite sulfate attack [3].

The presence of chloride in corrosive environments along with sulfates affects the interaction of both ions with the cement paste. Previous studies showed that sulfates inhibit chloride binding and chloride ingress [4, 5], as a result of the antagonism between sulfate and chloride ions to react with C_3A [6]. Moreover, the loss of stability of chloride-containing products due to the presence of sulfates [7] may lead to an increase of free chlorides in the pore solution [8].

Use of supplementary cementitious materials with pozzolanic properties is often suggested as a measure to improve the durability of concrete against aggressive environments [9–14]. Among others, metakaolin, a highly reactive calcined-clay admixture, can be included in the mix design, contributing in further reduction of concrete's CO_2 footprint. The Al-rich content of this mineral admixture contributes in chemical chloride binding which occurs through the formation of a complex chloroaluminate phase known as Friedel's salt ($3CaO{\cdot}Al_2O_3{\cdot}CaCl_2{\cdot}10H_2O$) [15], while the additional calcium silicate hydrate resulting from the pozzolanic reaction may contribute in physical binding of chlorides.

The present study investigates the effect of sulfates on the chloride ingress in Portland-limestone cement – metakaolin paste and relates it to the structural changes of cement hydrates, taking advantage of the capability of solid-state nuclear magnetic resonance (ssNMR) spectroscopy to assess both amorphous and crystalline phases. Free chlorides were directly determined and bound chlorides were indirectly assessed through the detection of Friedel's salt by X-ray powder diffraction (XRPD) analysis. The contribution of metakaolin in modifying the microstructure and chloride binding is highlighted by comparison to pure Portland-limestone cement paste. Cement pastes were intentionally used, to avoid any effect of the paste-aggregate interface.

2 Experimental

2.1 Materials and Exposure Conditions

Type CEM II/A-LL commercial Portland-limestone cement (PLC) and Mefisto L05 (ČLUZ, a.s.) metakaolin (MK) were used. Chemical composition of the raw materials is given in Table 1. PLC consisted of 56.5% C_3S, 13.1% C_2S, 7.0% C_3A, 9.4% C_4AF, 11.3% calcite, and 2.6 calcium sulfate minerals. MK consisted mainly of amorphous phase (92%) and, additionally, small amounts of quartz, hematite, anatase, phyllosilicates and mullite.

Pastes were produced from PLC and from a PLC/MK blend of 90:10 respective ratio (PLCMK) with a 0.45 water-to-binder ratio, and casted in the form of cylindrical

Table 1. Chemical composition (% w/w) of the raw materials.

Raw material	SiO_2	Al_2O_3	Fe_2O_3	CaO	TiO_2	SO_3	Other oxides
PLC	17.8	4.4	3.1	69.4	0.3	2.8	2.2
MK	52.5	42.7	1.1	0.6	1.8	0.1	1.2

specimens (d = 30 mm; h = 30 mm). The MK substitution level was selected according to literature data, suggesting optimal performance against sulfate attack [16]. After the 28-day initial curing period (24 h in the molds; 27 days immersed in water), the specimens (two from each binder) were introduced in the solutions shown in Table 2 and stored at 5 °C for 5 months.

Table 2. Exposure solutions and ions concentrations.

Code	Type	SO_4^{2-} (g/L)	Cl^- (g/L)
S0C20	chloride	0	21.14
S20C20	sulfate-chloride	20	21.14

Prior to exposure, a water-proof coating was applied on the surfaces of the specimens, leaving only the top circular one uncovered.

2.2 Tests

After the 5-month storage period, the specimens from each composition/solution were sliced at 5 mm, 10 mm and 15 mm, starting from the uncovered surface, and powdered by hand in an agate mortar to a maximum particle size of 63 μm. The powders (twelve samples) were used for XRPD analysis, determination of free chlorides, and ssNMR spectroscopy investigations.

XRPD data were collected with a Bruker D8 Advance diffractometer [CuK_α radiation ($\lambda = 1.5418$ Å)] in the angular range 5–80° 2θ, at 40 kV and 40 mA. Rietveld refinements of the XRPD patterns were performed with the TOPAS 4.2 software (Bruker AXS), providing quantitative phase analysis. The internal standard method was applied for determining the amorphous fraction.

Free (water-soluble) chloride contents were quantified in the powder sample produced from each depth interval (0–5 mm; 5–10 mm; 10–15 mm), using the ion exchange chromatograph Dionex ISC 5000 (ThermoFischer Scientific, USA) equipped with analytical column IonPac AS 22 (ThermoFischer Scientific, USA) and conductivity detector. To this aim, samples of 0.5 g in mass were placed in beakers filled up with ca. 95 mL of deionized water and kept stirring for 1 h. After 23 h, filtration of the water extracts was performed into 100 mL volumetric flasks that were brought to volume before chromatographic analysis. The measurements were accomplished using a solution composed of 4.5 mM Na_2CO_3 and 1.4 mM $NaHCO_3$ as mobile phase (flow rate of 1.2 mL/min).

One-pulse NMR spectra were collected with a Bruker Avance III 400 WB NMR spectrometer (Bruker, Billerica, MA, USA) at constant magnetic field of 9.4 T. ^{27}Al and ^{29}Si nuclei were characterized by the respective Larmor frequencies of 104.3 and 79.5 MHz. A 4-mm CP/MAS probe capable to rotate the samples at the magic angle to the direction of the constant magnetic field (stabilization accuracy of the rotation frequency ± 4 Hz) and stabilize their temperature (temperature stabilization accuracy ± 1 ºC) was used. Powder samples were loaded on a 4 mm zircon oxide rotor and rotated at 14 kHz (^{27}Al nuclei) or 12.5 kHz (^{29}Si nuclei). 1 M D_2O $AlCl_3$ solution and liquid tetramethylsilane were used as external references for ^{27}Al and ^{29}Si nuclei, respectively. The measurements were performed at 25 °C, recording 1024 scans with 4.5 μs pulse length and 2 s relaxation delay, in the case of ^{27}Al spectra. For ^{29}Si spectra, 8192 scans were recorded with 2.5 μs pulse length and 4 s relaxation delay.

3 Results and Discussion

Chloride ingress was assessed through the content of free chlorides and Friedel's salt at different depths. Figure 1 (left) illustrates that free chloride content was reduced in the samples of both compositions and for both exposure conditions for increasing depth. The decrease was steeper in the case of PLCMK composition, in which the overall contents were also lower than those determined in PLC. This is attributed to the denser microstructure resulting from the use of the MK admixture. Exposure to the combined solution S20C20 resulted, in general, in higher free chloride ion contents. This is more apparent for PLCMK, especially close to the surface (depth range 0–5 mm).

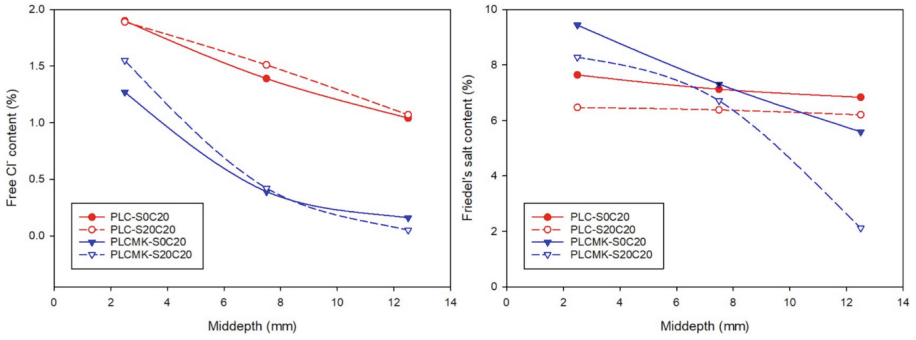

Fig. 1. Free chloride ions (left) and Friedel's salt (right) contents at different depths in PLC and PLCMK pastes after exposure to S0C20 and S20C20 solutions.

Similarly, Friedel's salt contents (Fig. 1 (right)) decreased with increasing the distance from specimens' surface, independently of cement paste composition and storage solution, however, the reduction was negligible in PLC paste. Friedel's salt content was higher in PLCMK at 0–5 mm, then became almost equal for both compositions at the depth range 5–10 mm, while significant decrease at 10–15 mm was observed for PLCMK. The presence of sulfate ions (S20C20) led to decreased Friedel's salt contents in the specimens of both compositions, compared to S0C20 solution.

Quantitative results for ettringite and portlandite are reported in Fig. 2.

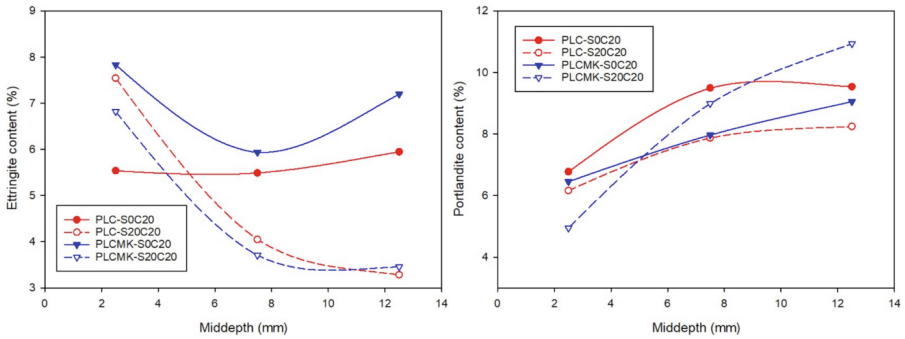

Fig. 2. Ettringite (left) and portlandite (right) contents at different depths in PLC and PLCMK pastes after exposure to S0C20 and S20C20 solutions.

In the case of exposure to S0C20 solution, ettringite content (Fig. 2 (left)) shows an increasing trend at depths above 5 mm, contrary to those of Friedel's salt (Fig. 1 (right)). Storage in S20C20 solution resulted in noticeable higher contents at the depth range 0–5 mm in both PLC and PLCMK pastes. This observation can be related to the reduced portlandite content at this depth range (Fig. 2 (right)), that apparently was leached and consumed towards ettringite formation [16]. At higher depths (5–10 mm and 10–15 mm), the ettringite content in both pastes exposed to the combined solution, is reduced, thus, it can be considered as the ettringite formed during hydration.

^{27}Al MAS NMR spectra of all the samples are characterized by two signals centered at ca. 10.5 ppm and 15.0 ppm (Fig. 3). They are attributed to Al in octahedral coordination, corresponding to Friedel's salt and ettringite, respectively [17, 18]. In all the PLC samples, the intensity of the component at 15.0 ppm was always higher than that at 10.5 ppm. The stability of the intensity of the latter component correlates well with the substantially constant Friedel's salt content in these samples (Fig. 1 (right)). In the PLCMK samples the intensity of the two peaks was strongly dependent on the depth from the surface. At 10–15 mm, significant reduction of the intensity of the component at 10.5 ppm was observed, in agreement with the reduction of Friedel's salt content derived from XRPD analysis. For both compositions, the intensity of the signal corresponding to Friedel's salt (at 10.5 ppm) was always lower for the specimens stored in S20C20 solution, compared to S0C20. An additional broad component of low intensity was observed in all the samples of PLCMK paste at ca. 74.0 ppm (not shown here for figure's simplicity), which is characteristic for AlO_4 tetrahedra incorporated in C–S–H phase [19].

Representative ^{29}Si MAS NMR spectra are illustrated in Fig. 4.

The main signals correspond to Q^2 (–84 ppm), Q^2(1Al) (–81 ppm), Q^1 (–79 ppm) and Q^0 (–74 and –71 ppm) silicon species [20]. Larger quantity of unreacted clinker phases and more extensive incorporation of Al in C–S–H differentiate the spectra of PLCMK samples from those of PLC. A comparison between the PLC paste stored in S0C20 and S20C20 reveals that the paste was hydrated at a greater degree in the chloride solution,

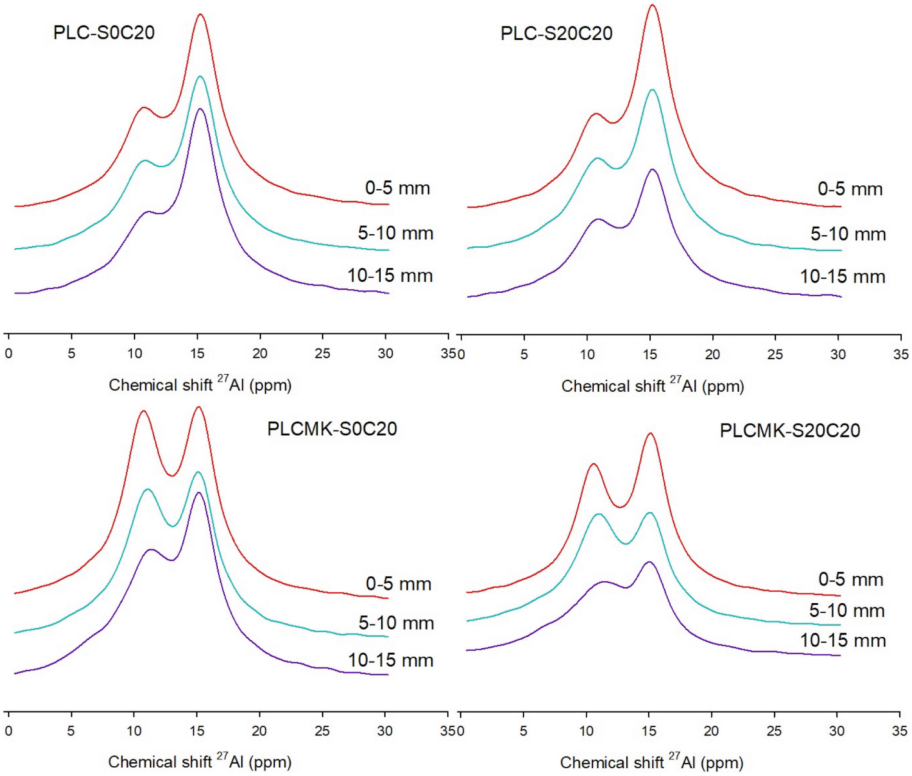

Fig. 3. ^{27}Al MAS NMR spectra obtained at different depths in PLC and PLCMK pastes after exposure to S0C20 and S20C20 solutions.

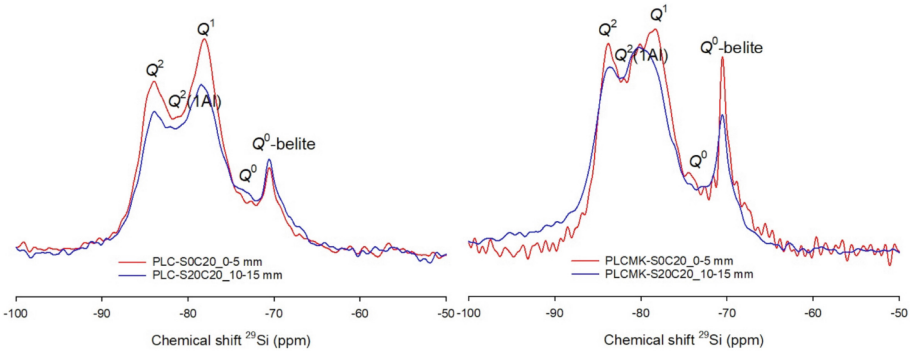

Fig. 4. ^{29}Si MAS NMR spectra obtained at different depths in PLC and PLCMK pastes after exposure to S0C20 and S20C20 solutions.

independently of the depth, while the polymerization of silicate chains in the C–S–H phase, based on the proportion of the intensity of Q^2 and Q^1 species, is mostly similar in all the PLC samples. Polymerization in the PLCMK samples is higher at 0–5 mm, as indicated by the increased intensity of Q^2 species, which, contrary to PLC paste, decreased with depth increase. The presence of sulfates along with chlorides reduced the intensity of the signal of Q^2 species in PLCMK samples.

4 Conclusions

The study provided information about the effect of sulfates on chloride ingress and microstructure in Portland-limestone cement – metakaolin paste, highlighting also the influence of the pozzolanic admixture. The use of MK in the blend differentiated the cement paste characteristics, increasing the availability of Al to bind chlorides and incorporate in the C–S–H phase. Close to the surface, the silicate chains of C–S–H became more extensively polymerized, while larger amounts of clinker remained unreacted. At higher depths, chlorides bound in the form of Friedel's salt and free chlorides, were considerably reduced, attributed to refinement of the matrix. Furthermore, less polymerization of C–S–H was observed and less unreacted clinker phases were detected. The presence of sulfates in the exposure solution affected chloride binding by inhibiting the formation of Friedel's salt and increasing free chlorides in the pore solution. Moreover, sulfates decreased the polymerization of the silicate chains in C–S–H of the Portland-limestone cement – metakaolin paste and inhibited the hydration of clinker in pure Portland-limestone cement paste.

Acknowledgements. The work was funded by the Czech Science Foundation (grant number 21-35772J) and the Russian Foundation for Basic Research (grant number 20–52-26021).

References

1. EN 197–1, Cement – Part 1: Composition, specifications and conformity criteria for common cements, CEN/TC 51/WG 6, Brussels (2011)
2. ASTM C595/C595M-12, Standard specification for blended hydraulic cement, West Conshohocken, PA, USA (2012)
3. Bensted, J.: Thaumasite – background and nature in deterioration of cement mortars and concretes. Cement Concr. Compos. **21**(2), 117–121 (1999)
4. Frias, M., Goñi, S., García, R., de La Villa, R.V.: Seawater effect on durability of ternary cements: Synergy of chloride and sulphate ions. Compos. B Eng. **46**, 173–178 (2013)
5. Chen, Y., Gao, J., Tang, L., Li, X.: Resistance of concrete against combined attack of chloride and sulfate under drying-wetting cycles. Constr. Build. Mater. **106**, 650–658 (2016)
6. Luo, R., Cai, Y., Wang, C., Huang, X.: Study of chloride binding and diffusion in GGBS concrete. Cem. Concr. Res. **33**(1), 1–7 (2003)
7. De Weerdt, K., Orsáková, D., Geiker, M.R.: The impact of sulphate and magnesium on chloride binding in Portland cement paste. Cem. Concr. Res. **65**, 30–40 (2014)
8. Ehtesham Hussain, S., Al-Gahtani, A.S.: Influence of sulfates on chloride binding in cements. Cem. Concr. Res. **24**(1), 8–24 (1994)

9. Sotiriadis, K., Nikolopoulou, E., Tsivilis, S., Pavlou, A., Chaniotakis, E., Swamy, R.N.: The effect of chlorides on the thaumasite form of sulfate attack of limestone cement concrete containing mineral admixtures at low temperature. Constr. Build. Mater. **43**, 156–164 (2013)
10. Sotiriadis, K., Tsivilis, S.: Performance of limestone cement concretes in chloride-sulfate environments at low temperature. Mag. Concr. Res. **70**(20), 1039–1051 (2018)
11. Sotiriadis, K., Rakanta, E., Mitzithra, M.E., Batis, G., Tsivilis, S.: Chloride-related phenomena in limestone cement materials: Effect of mineral admixtures and sulfates. ACI Mater. J. **116**(6), 19–30 (2019)
12. Hossain, M.M., Karim, M.R., Hasan, M., Hossain, M.K., Zain, M.F.M.: Durability of mortar and concrete made up of pozzolans as a partial replacement of cement: A review. Constr. Build. Mater. **116**, 128–140 (2016)
13. Rahman, M.M., Bassuoni, M.T.: Thaumasite sulfate attack on concrete: Mechanisms, influential factors and mitigation. Constr. Build. Mater. **73**, 652–666 (2014)
14. Shi, X., Xie, N., Fortune, K., Gong, J.: Durability of steel reinforced concrete in chloride environments: An overview. Constr. Build. Mater. **30**, 125–138 (2012)
15. Baroghel-Bouny, V., Wang, X., Thiery, M., Sailio, M., Barberon, F.: Prediction of chloride binding isotherms of cementitious materials by "analytical" model or "numerical" inverse analysis. Cem. Concr. Res. **42**(9), 1207–1224 (2012)
16. Siddique, R., Klaus, J.: Influence of metakaolin on the properties of mortar and concrete: A review. Appl. Clay Sci. **43**(3–4), 392–400 (2009)
17. Matschei, T., Lothenbach, B., Glasser, F.P.: The role of calcium carbonate in cement hydration. Cem. Concr. Res. **37**(4), 551–558 (2007)
18. Jones, M.R., et al.: Studies using 27Al MAS NMR of AFm and Aft phases and the formation of Friedel's salt. Cem. Concr. Res. **33**(2), 177–182 (2003)
19. Barberon, F., et al.: Interactions between chloride and cement-paste materials. Mag. Resonance Imaging **23**(2), 267–272 (2005)
20. Andersen, M.D., Jakobsen, H.J., Skibsted, J.: Incorporation of aluminum in the calcium silicate hydrate (C-S-H) of hydrated Portland cements: A high-field ^{27}Al and ^{29}Si MAS NMR investigation. Inorg. Chem. **42**(7), 2280–2287 (2003)
21. Walkley, B., Provis, J.L.: Solid-state nuclear magnetic resonance spectroscopy of cements. Materials Today Adv. **1**, 100007 (2019)